A Novel Algebraic Scheme for Describing Coupled Benders in Tetratomic Molecules†

F. Iachello‡,§ and F. Pérez-Bernal*,||

Center for Theoretical Physics, Sloane Physics Laboratory, Yale University, P.O. Box 208120, New Haven, Connecticut 06520-8120, Department of Chemistry, Yale University, P.O. Box 208107, New Haven, Connecticut 06520-8107, and Depto. de Física Aplicada, Fac. de Ciencias Experimentales, Universidad de Huelva, Campus del Carmen, Avda. de las Fuerzas Armadas s/n, 21071 Huelva, Spain

Received: May 1, 2009; Revised Manuscript Received: July 4, 2009

An algebraic scheme for describing the bending dynamics of tetratomic molecules including linear, bent planar, and bent a-planar species is introduced. The correlation diagram linear−cis-bent and linear−trans-bent is constructed. Effective potential energy functions are evaluated by exploiting the method of coherent states. A sample calculation of the bending vibrations of C_2H_2 in its $\tilde{X}^1\Sigma_g^+$ electronic ground state is performed.

1. Introduction

Coupled benders provide an interesting window into the many facets of molecular dynamics. In tetratomic molecules, for example, several geometric configurations are possible: linear, cis-bent, trans-bent and nonplanar, as schematically depicted in Figure 1 for symmetric ABBA molecular species.

In addition, molecular species exist with a nonrigid structure, intermediate between the four configurations of Figure 1. A description of all configurations (rigid and nonrigid) within the framework of a single approach is very challenging. Most approaches so far have concentrated on linear or quasi-linear geometries. Noteworthy are the force-field approach of Strey and Mills to linear HCCH[1,2] and the use of Dunham-type expansion plus resonance terms.[3,4] Within the algebraic methodology, the approaches to the combined rotation−vibration spectra of linear, HCCH, HCCD, DCCD,[5] HCCF,[6,7] and quasi-linear, HCNO[8] molecules, as well as to the purely vibrational spectrum of HCCH[9] are also worthy of notice. All approaches require a large number of parameters for an accurate description of all vibrational and rotational levels.

Much insight into the structure of tetratomic molecules can be obtained by an analysis of pure-bend levels, i.e. two coupled benders. These have been analyzed recently for linear molecules in the Dunham-type expansion plus resonances approach,[3,4] in the force field expansion approach[2,10] and with semiclassical methods.[11,12]

In this article, we introduce a novel algebraic scheme for describing coupled benders and show that already with a Hamiltonian quadratic in the elements of the algebra (and thus with few parameters) we can describe all situations depicted in Figure 1. This scheme builds on the algebraic approach to benders (two-dimensional problems) of Iachello and Oss[13] in terms of the Lie algebra $U(3)$ (single bender) and $U(3) \otimes U(3)$ (coupled benders), extended to nonrigid single benders in refs 14 and 15 and analyzed from the point of view of quantum phase transitions in refs 16 and 17. The approach of ref 13 was already extended to nonplanar molecules (H_2O_2) in ref 18. The novel scheme presented in this article includes this extension as a special case, since the interaction used in ref 18 to generate spectra of nonplanar molecules is the quadrupole interaction $\hat{Q}_1 \cdot \hat{Q}_2$ which is part of our Hamiltonian equation (10). However, it is more general, since, within the same framework, it can describe all configurations of Figure 1, linear, cis-bent, trans-bent and nonplanar. Cis-bent and trans-bent configurations had not been treated previously within the algebraic approach.

To show that the new scheme can treat all cases, we construct potential energy surfaces corresponding to our algebraic Hamiltonian as a function of the dihedral angle ϕ and show that they support equilibrium configurations which are either linear ($r_e = 0$), or cis-bent ($r_e \neq 0$, $\phi = 0$), or trans-bent ($r_e \neq 0$, $\phi = \pi$), or nonplanar ($r_e \neq 0$, $\phi \neq 0, \pi$).

As a sample calculation we perform fits to the lowest 53 observed pure-bend levels of the ground electronic state of HCCH, $\tilde{X}^1\Sigma^+$. A fit with a quadratic Hamiltonian with 3 parameters yields a rms deviation of 17.1 cm^{-1} while a fit with 7 parameters yields a rms of 6.1 cm^{-1}.

Our purpose in this article is to show what are the salient features of the bending spectra of tetratomic molecules, and that these features can be obtained with a limited number of parameters. In ref 9, the bending spectra of HCCH in its ground electronic state were studied. In addition to the 7 linear and quadratic terms that we have included, the authors of ref 9 included also two cubic and three quartic terms. These terms bring down the rms deviation to spectroscopic accuracy, 0.06 cm^{-1}. Although we can easily introduce these terms, since they are powers or products of the operators discussed in the section below, we have not done so in this article, as our intention was to present the general formalism and show that within this formalism we can produce cis-bent, trans-bent, and nonplanar configurations in addition to the linear configuration of ref 13. Higher order terms can be introduced in a systematic fashion in the algebraic approach as discussed in ref 19.

Within the framework of the algebraic approach it is also possible to study intensities of infrared and Raman transitions. A general way to construct the corresponding operators is given in ref 19. For bending vibrations, the infrared operator were introduced in ref 13 and the matrix elements calculated in ref 18. Matrix elements of these operators can be calculated also for the novel algebraic scheme and will be the subject of a subsequent investigation.

† Part of the "Robert W. Field Festschrift".

* Corresponding author.
‡ Center for Theoretical Physics, Sloane Physics Laboratory, Yale University.
§ Department of Chemistry, Yale University.
|| Universidad de Huelva.

10.1021/jp9040474 CCC: $40.75
Published on Web 08/27/2009

2. Algebra for Coupled Benders

We begin by reviewing the algebraic approach to coupled benders of ref 13.

2.1. Bosonic $U_1(3) \otimes U_2(3)$ Algebra for Coupled Benders. Each bender (2D system) is described by a U(3) algebra constructed from bilinear products of boson creation ($\tau_x^\dagger$, $\tau_y^\dagger$, $\sigma^\dagger$) and annihilation (τ_x, τ_y, σ) operators. For two benders ($\tau_{x,s}^\dagger$, $\tau_{y,s}^\dagger$, $\sigma_s^\dagger$), ($\tau_{x,s}$, $\tau_{y,s}$, σ_s), $s = 1, 2$. The boson operators satisfy the usual commutation relations

$$[\sigma_i,\sigma_j^\dagger] = \delta_{i,j} \qquad [\tau_{\alpha,i},\tau_{\beta,j}^\dagger] = \delta_{i,j}\delta_{\alpha,\beta} \tag{1}$$

where $i, j = 1, 2$, $\alpha, \beta = x, y$, and all other commutators zero.

The $18 = 9 + 9$ bilinear products of creation and annihilation operators of the same species, $s = 1$ or $s = 2$, generate the Lie algebra $U_1(3) \otimes U_2(3)$. It is convenient to introduce circular boson operators

$$\tau_{\pm,j}^\dagger = \mp\frac{\tau_{x,j}^\dagger \pm i\tau_{y,j}^\dagger}{\sqrt{2}} \tag{2a}$$

$$\tau_{\pm,j} = \mp\frac{\tau_{x,j} \mp i\tau_{y,j}}{\sqrt{2}} \qquad j = 1, 2 \tag{2b}$$

Our choice of phases (different from ref 13) is the same as in ref 16. Circular bosons have also been used in the force field expansion of ref 10.

It is convenient to denote the bilinear products as[13]

$$\begin{array}{ll}
\hat{n}_j = \tau_{+,j}^\dagger\tau_{+,j} + \tau_{-,j}^\dagger\tau_{-,j} & \hat{n}_{\sigma,j} = \sigma_j^\dagger\sigma_j \\
\hat{l}_j = \tau_{+,j}^\dagger\tau_{+,j} - \tau_{-,j}^\dagger\tau_{-,j} & \\
\hat{D}_{+,j} = \sqrt{2}(\tau_{+,j}^\dagger\sigma_j - \sigma_j^\dagger\tau_{-,j}) & \hat{D}_{-,j} = \sqrt{2}(-\tau_{-,j}^\dagger\sigma_j + \sigma_j^\dagger\tau_{+,j}) \\
\hat{Q}_{+,j} = \sqrt{2}\tau_{+,j}^\dagger\tau_{-,j} & \hat{Q}_{-,j} = \sqrt{2}\tau_{-,j}^\dagger\tau_{+,j} \\
\hat{R}_{+,j} = \sqrt{2}(\tau_{+,j}^\dagger\sigma_j + \sigma_j^\dagger\tau_{-,j}) & \hat{R}_{-,j} = \sqrt{2}(\tau_{-,j}^\dagger\sigma_j + \sigma_j^\dagger\tau_{+,j})
\end{array} \tag{3}$$

where $j = 1, 2$.

Starting from the algebraic structure $U_1(3) \otimes U_2(3)$, it is possible to list all the possible dynamical symmetries (i.e., situations in which the energy eigenvalues can be written in explicit form in terms of quantum numbers) of the coupled systems. This list is given in ref 13. We split it here into six, conserving total 2D angular momentum and relevant to ABBA molecules,

$$\begin{array}{lcl}
 & & SO_1(2)\otimes SO_2(2) \quad \text{(Ia)} \\
 & & \quad / \qquad \backslash \\
U_1(3)\otimes U_2(3) & \supset & U_1(2)\otimes U_2(2) \qquad SO_{12}(2), \\
 & & \quad \backslash \qquad / \\
 & & \quad U_{12}(2) \quad \text{(Ib)}
\end{array}$$

$$\begin{array}{lcl}
 & & SO_1(2)\otimes SO_2(2) \quad \text{(IIa)} \\
 & & \quad / \qquad \backslash \\
U_1(3)\otimes U_2(3) & \supset & SO_1(3)\otimes SO_2(3) \qquad SO_{12}(2), \\
 & & \quad \backslash \qquad / \\
 & & \quad SO_{12}(3) \quad \text{(IIb)}
\end{array} \tag{4}$$

$$\begin{array}{lcl}
 & & U_{12}(2) \quad \text{(IIIa)} \\
 & & \quad / \qquad \backslash \\
U_1(3)\otimes U_2(3) & \supset & U_{12}(3) \qquad SO_{12}(2), \\
 & & \quad \backslash \qquad / \\
 & & \quad SO_{12}(3) \quad \text{(IIIb)}
\end{array}$$

and one, relevant to molecules with inequivalent benders

$$U_1(3) \otimes U_2(3) \supset U_1(2) \otimes SO_2(3) \supset SO_1(2) \otimes SO_2(2) \supset SO_{12}(2) \quad \text{(IV)} \tag{5}$$

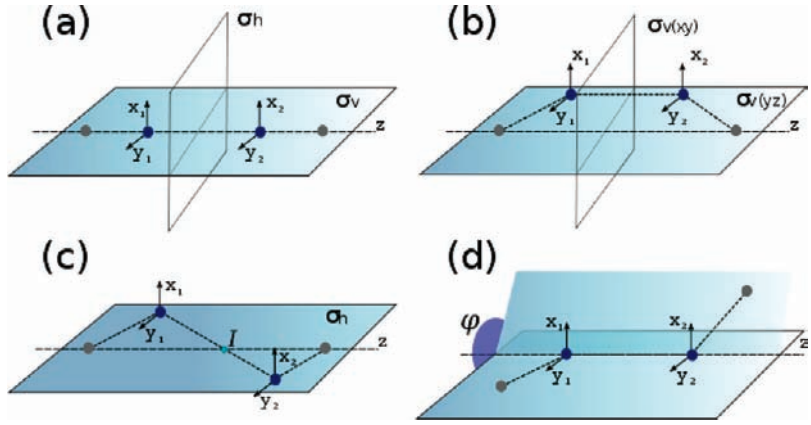

Figure 1. Schematic representation of the four geometrical configurations of ABBA tetratomic molecules: (a) linear; (b) cis-bent; (c) trans-bent; (d) nonplanar.

which we will not consider in this article. The symmetries Ia and IIa describe uncoupled benders, either linear (Ia) or bent (IIa). They can be conveniently used to generate a basis for calculation. This basis is often denoted as *local* basis. The symmetries Ib and IIb describe coupled benders, either linear (Ib) or bent (IIb). The chains IIIa and IIIb describe normal benders.[19]

Each of the choices in eq 4 contains subalgebras of $U_1(3) \otimes U_2(3)$, with elements

$$\begin{array}{ll} U_{12}(3) & \{\hat{n}_{12},\hat{l}_{12},\hat{D}_{+,12},\hat{D}_{-,12},\hat{R}_{+,12},\hat{R}_{-,12},\hat{Q}_{+,12},\hat{Q}_{-,12}\} \\ U_{12}(2) & \{\hat{n}_{12},\hat{l}_{12},\hat{Q}_{+,12},\hat{Q}_{-,12}\} \\ U_i(2) & \{\hat{n}_i,\hat{l}_i,\hat{Q}_{+,i},\hat{Q}_{-,i}\}, \quad i = 1,2 \\ SO_i(3) & \{\hat{l}_i,\hat{D}_{+,i},\hat{D}_{-,i}\}, \quad i = 1,2 \\ SO_{12}(3) & \{\hat{l}_{12},\hat{D}_{+,12},\hat{D}_{-,12}\} \\ SO_i(2) & \{\hat{l}_i\}; \quad i = 1,2 \\ SO_{12}(2) & \{\hat{l}_{12}\} \end{array} \tag{6}$$

where the subindex 12 stands for the operator sum, e.g., $\hat{n}_{12} = \hat{n}_1 + \hat{n}_2$.

2.2. Hamiltonian. A generic Hamiltonian within the model space of the previous subsection 2.1 can be constructed by considering the invariant Casimir operators of all subalgebras in eq 4,

$$\begin{array}{ll} \hat{C}_1[U_i(2)] = \hat{n}_i & \hat{C}_2[U_i(2)] = \hat{n}_i(\hat{n}_i + 1), \quad i = 1,2 \\ \hat{C}_1[U_{12}(2)] = \hat{n}_{12} & \hat{C}_2[U_{12}(2)] = (\hat{n}_{12}^2 + \hat{l}_{12}^2 + \hat{n}_1^2 + \hat{n}_2^2 - \hat{l}_1^2 - \hat{l}_2^2)/2 + \hat{Q}_1\cdot\hat{Q}_2 \\ \hat{C}_1[U_{12}(3)] = \hat{n}_{12} + \hat{n}_{\sigma,12} = \hat{N}_{12} & \hat{C}_2[U_{12}(3)] = \hat{M}_{12} = \hat{n}_1\hat{n}_{\sigma,2} + \hat{n}_2\hat{n}_{\sigma,1} - \hat{D}_1\cdot\hat{D}_2 - \hat{R}_1\cdot\hat{R}_2 \\ \hat{C}_2[SO_i(3)] = \hat{W}_i^2 = (\hat{D}_{+,i}\hat{D}_{-,i} + \hat{D}_{-,i}\hat{D}_{+,i})/2 + \hat{l}_i^2, \quad i = 1,2 & \\ \hat{C}_1[SO_i(2)] = \hat{l}_i & \hat{C}_2[SO_i(2)] = \hat{l}_i^2, \quad i = 1,2 \\ \hat{C}_2[SO_{12}(3)] = \hat{W}_{12}^2 = (\hat{D}_{+,12}\hat{D}_{-,12} + \hat{D}_{-,12}\hat{D}_{+,12})/2 + \hat{l}_{12}^2 & \\ \hat{C}_1[SO_{12}(2)] = \hat{l}_{12} & \hat{C}_2[SO_{12}(2)] = \hat{l}_{12}^2 \end{array} \tag{7}$$

The most general Hamiltonian up to terms which are quadratic in the elements of the algebra is

$$\begin{aligned} \hat{H} = {} & E_0 + \sum_{i=1}^{2}\{e_i\hat{C}_1[U_i(2)] + a_i\hat{C}_2[U_i(2)] + b_i\hat{C}_2[SO_i(2)] + c_i\hat{C}_2[SO_i(3)]\} + \\ & a_{12}\hat{C}_1[U_1(2)]\,\hat{C}_1[U_2(2)] + b_{12}\hat{C}_2[SO_{12}(2)] + c_{12}\hat{C}_2[SO_{12}(3)] + \\ & e_{12}\hat{C}_1[U_{12}(2)] + d_{12}\hat{C}_2[U_{12}(2)] + f_{12}\hat{C}_2[U_{12}(3)] \end{aligned} \tag{8}$$

where the term $\hat{C}_1[U_{12}(3)]$ has been absorbed into E_0 since it is a constant. This Hamiltonian has 14 parameters. For ABBA molecules, the two benders are equivalent and symmetry considerations reduce the number of parameters to 9,

$$\begin{aligned}\hat{H} \;=\; & E_0 + e\sum_{i=1}^{2}\hat{C}_1[\mathrm{U}_i(2)] + a\sum_{i=1}^{2}\hat{C}_2[\mathrm{U}_i(2)] + \\ & b\sum_{i=1}^{2}\hat{C}_2[\mathrm{SO}_i(2)] + c\sum_{i=1}^{2}\hat{C}_2[\mathrm{SO}_i(3)] + \\ & a_{12}\hat{C}_1[\mathrm{U}_1(2)]\,\hat{C}_1[\mathrm{U}_2(2)] + b_{12}\hat{C}_2[\mathrm{SO}_{12}(2)] + c_{12}\hat{C}_2[\mathrm{SO}_{12}(3)] + \\ & d_{12}\hat{C}_2[\mathrm{U}_{12}(2)] + f_{12}\hat{C}_2[\mathrm{U}_{12}(3)]\end{aligned} \tag{9}$$

Rather than using the abstract form eq 9, it is convenient to rewrite it in terms of operators with physical meaning

$$\begin{aligned}\hat{H} \;=\; & E_0' + \varepsilon(\hat{n}_1 + \hat{n}_2) + \\ & \alpha[\hat{n}_1(\hat{n}_1 + 1) + \hat{n}_2(\hat{n}_2 + 1)] + \alpha_{12}\hat{n}_1\hat{n}_2 + \\ & \beta(\hat{l}_1^{\,2} + \hat{l}_2^{\,2}) + \beta_{12}\hat{l}_1\hat{l}_2 + \\ & \lambda(\hat{D}_1\cdot\hat{D}_2 + \hat{R}_1\cdot\hat{R}_2) + B\hat{Q}_1\cdot\hat{\mathrm{Q}} + \\ & A(\hat{W}_1^{\,2} + W_2^{\,2}) + A_{12}\hat{W}_1\cdot\hat{W}_2\end{aligned} \tag{10}$$

Equation 10 represents the algebraic expansion of the Hamiltonian up to order 2. The first 5 terms (ε, α, α_{12}, β, β_{12}) are diagonal in the local basis (Dunham-like expansion) while the last four (λ, B, A, A_{12}) represent the correlations that induce local to normal transitions (λ), and linear to bent (B, A, A_{12}).

2.3. Limiting Cases and Basis for Diagonalization. It is of interest to investigate the six dynamical symmetries (Ia, Ib, IIa, IIb, IIIa, IIIb) of the Hamiltonian of eq 4. For the sake of conciseness we consider in this article only two, Ia and IIa, which provide the basis for the numerical diagonalization of the Hamiltonian.

2.3.1. Dynamical Symmetry Ia. This limiting case is of particular importance, since it provides the most convenient basis for numerical diagonalization of the Hamiltonian operator. The basis states are labeled by

$$\left|\begin{matrix}\mathrm{U}_1(3) & \otimes & \mathrm{U}_2(3) & \supset & \mathrm{U}_1(2) & \otimes & \mathrm{U}_2(2) & \supset & \mathrm{SO}_1(2) & \otimes & \mathrm{SO}_2(2) & \supset & \mathrm{SO}_{12}(2) \\ [N_1] & & [N_2] & & n_1 & & n_2 & & l_1 & & l_2 & & (l_{12})\end{matrix}\right\rangle \tag{11}$$

The quantum number $l_{12} = l_1 + l_2$ has been placed in parentheses since it is not independent of the others. The quantum numbers N_i (vibron numbers) label the totally symmetric representations of $\mathrm{U}_i(3)$, i.e., the dimension of the space in which the calculation is done. The quantum numbers n_i denote the local vibrational quantum number and l_i is the 2D angular momentum for each cylindrical oscillator, with $i = 1, 2$. The quantum number l_{12} is the coupled 2D angular momentum, $l_{12} = l_1 + l_2$. We call the basis associated with chain Ia the *local* basis.

The branching rules are

$$\begin{aligned}& n_i = N_i, N_i - 1, N_i - 2, ..., 0 \\ & l_i = \pm n_i, \pm(n_i - 2), ..., \pm 1 \text{ or } 0\ (n_i = \text{odd or even})\end{aligned} \tag{12}$$

where $i = 1, 2$.

This limiting case corresponds to taking $\lambda = B = A = A_{12} = 0$ in eq 10. The energy eigenvalues are

$$E^{(\mathrm{Ia})}(n_1,l_1,n_2,l_2) = E_0 + \varepsilon\sum_{i=1}^{2}n_i + \alpha\sum_{i=1}^{2}n_i(n_i + 1) + \alpha_{12}n_1n_2 + \beta\sum_{i=1}^{2}l_i^{\,2} + \beta_{12}l_1l_2 \tag{13}$$

In eq 13 the labels N_1 and N_2 have been dropped and l_{12} has been omitted since it is equal to $l_1 + l_2$. The basis states can be written as

$$|n_1^{l_1},n_2^{l_2}\rangle = \prod_{i=1}^{2}\frac{(\sigma_i^\dagger)^{N_i-n_i}(\tau_{i,+}^\dagger)^{(n_i+l_i)/2}(\tau_{i,-}^\dagger)^{(n_i-l_i)/2}}{\sqrt{(N_i - n_i)!\left(\frac{n_i + l_i}{2}\right)!\left(\frac{n_i - l_i}{2}\right)!}}|0\rangle \tag{14}$$

where the compact spectroscopic notation $|n_1^{l_1}, n_2^{l_2}\rangle$ has been used.

This dynamical symmetry corresponds to two local uncoupled linear benders.

2.3.2. Dynamical Symmetry IIa. The basis states are labeled by

$$\left|\begin{matrix}\mathrm{U}_1(3) & \otimes & \mathrm{U}_2(3) & \supset & \mathrm{SO}_1(3) & \otimes & \mathrm{SO}_2(3) & \supset & \mathrm{SO}_1(2) & \otimes & \mathrm{SO}_2(2) & \supset & \mathrm{SO}_{12}(2) \\ [N_1] & & [N_2] & & \omega_1 & & \omega_2 & & l_1 & & l_2 & & (l_{12})\end{matrix}\right\rangle \tag{15}$$

The branching rules are

$$\omega_i = N_i, N_i - 2, N_i - 4, ..., 1 \text{ or } 0 \quad (N_i = \text{odd or even}); \qquad i = 1, 2$$
$$l_i = \pm\omega_i, \pm(\omega_i - 1), ..., \pm 1, 0; \qquad i = 1,2 \quad (16)$$

As in the dynamical symmetry Ia, the l_{12} label can be omitted. It is convenient to introduce a vibrational quantum number v_i, which can be identified with the number of quanta of excitation in the ith displaced oscillator:

$$v_i = \frac{N_i - \omega_i}{2} \quad (17)$$

The branching rules in terms of v_i are

$$v_i = 0, 1, ..., \frac{N_i - 1}{2} \text{ or } \frac{N_i}{2} \ (N_i = \text{odd or even})$$
$$l_i = 0, \pm 1, \pm 2, ..., \pm(N_i - 2v_i); \qquad i = 1, 2 \quad (18)$$

This limiting case corresponds to taking $\varepsilon = \alpha = \alpha_{12} = \lambda = A_{12} = B = 0$ in eq 10. The energy eigenvalues are

$$E^{(\mathrm{IIa})}(v_1,v_2,l_1,l_2) = E_0 - 4A\sum_{i=1}^{2}[(N_i + 1/2)v_i - v_i^2] \quad (19)$$

$$+ \beta\sum_{i=1}^{2} l_i^2 + b_{12}l_1l_2$$

This dynamical symmetry corresponds to two local uncoupled displaced benders.

2.4. Operator Matrix Elements. To diagonalize the Hamiltonian of eq 10 in the local basis (Ia), one needs the matrix elements of those operators that are nondiagonal, that is, $\hat{D}_1\cdot\hat{D}_2 + \hat{R}_1\cdot\hat{R}_2$, $\hat{Q}_1\cdot\hat{Q}_2$, $(\hat{W}_1^2 + \hat{W}_2^2)$, and $\hat{W}_1\cdot\hat{W}_2$.

2.4.1. Operator $\hat{D}_1\cdot\hat{D}_2 + \hat{R}_1\cdot\hat{R}_2$. Matrix elements of the $\hat{C}_2[U_{12}(3)]$ Casimir operator, called the Majorana operator, were given in ref 13. The operator $\hat{D}_1\cdot\hat{D}_2 + \hat{R}_1\cdot\hat{R}_2$ is part of the Majorana operator (see eq 7). Its matrix elements in the local basis are

$$\langle (n_1 - 1)^{l_1\mp 1}, (n_2 + 1)^{l_2\pm 1} | \hat{D}_1\cdot\hat{D}_2 + \hat{R}_1\cdot\hat{R}_2 | n_1^{l_1}, n_2^{l_2}\rangle = \sqrt{(N_1 - n_1 + 1)(N_2 - n_2)\left(\frac{n_1 \pm l_1}{2}\right)\left(\frac{n_2 \pm l_2}{2} + 1\right)} \quad (20)$$

and similar expressions with the index 1 interchanged with 2 on the left-hand side.

The operator $\hat{D}_1\cdot\hat{D}_2 + \hat{R}_1\cdot\hat{R}_2$ conserves the polyad number of Kellman[11,20] in a local approach and leads from local to normal behavior.[21] This operator, when viewed from the normal basis, induces Darling Dennison couplings as discussed in ref 19, p 94.

2.4.2. Quadrupole Interaction $\hat{Q}_1\cdot\hat{Q}_2$. The matrix elements of $\hat{Q}_1\cdot\hat{Q}_2$ are

$$\langle n_1^{l_1\pm 2}, n_2^{l_2\mp 2} | \hat{Q}_1\cdot\hat{Q}_2 | n_1^{l_1}, n_2^{l_2}\rangle = \sqrt{(n_1 \mp l_1)(n_2 \pm l_2)\left(\frac{n_1 \pm l_1}{2} + 1\right)\left(\frac{n_2 \mp l_2}{2} + 1\right)} \quad (21)$$

This operator is called vibrational l resonance in ref 3. It conserves the polyad number[22] in a local approach.

2.4.3. Operators $\hat{W}_1^2$ and $\hat{W}_2^2$. The diagonal matrix elements of $\hat{W}_1^2$ and $\hat{W}_2^2$ are

$$\langle n_1^{l_1}, n_2^{l_2} | \hat{W}_i^2 | n_1^{l_1}, n_2^{l_2}\rangle = 2N_i(n_i + 1) - (2n_i + 1)n_i + l_i^2 \quad (22)$$

The off-diagonal matrix elements are

$$\langle (n_i - 2)^{l_i}, n_j^{l_j} | \hat{W}_i^2 | n_i^{l_i}, n_j^{l_j}\rangle = -\sqrt{(N_i - n_i + 2)(N_i - n_i + 1)(n_i + l_i)(n_i - l_i)} \quad (23)$$

where $i, j = 1, 2$ and $i \neq j$.

The operators $\hat{W}_1^2$ and $\hat{W}_2^2$ lead from linear to bent. They do not preserve polyad number.

2.4.4. Operator $\hat{W}_1\cdot\hat{W}_2$. The diagonal matrix elements are

$$\langle n_1^{l_1}, n_2^{l_2} | \hat{W}_1\cdot\hat{W}_2 | n_1^{l_1}, n_2^{l_2}\rangle = l_1l_2 \quad (24)$$

while the off-diagonal matrix elements are

$$\langle (n_1 + 1)^{l_1+1}, (n_2 + 1)^{l_2-1} | \hat{W}_1\cdot\hat{W}_2 | n_1^{l_1}, n_2^{l_2}\rangle = -\sqrt{(N_1 - n_1)(N_2 - n_2)\left(\frac{n_1 + l_1}{2} + 1\right)\left(\frac{n_2 - l_2}{2} + 1\right)}$$

$$\langle (n_1 + 1)^{l_1+1}, (n_2 - 1)^{l_2-1} | \hat{W}_1\cdot\hat{W}_2 | n_1^{l_1}, n_2^{l_2}\rangle = \sqrt{(N_1 - n_1)(N_2 - n_2 + 1)\left(\frac{n_1 + l_1}{2} + 1\right)\left(\frac{n_2 + l_2}{2}\right)}$$

$$\langle (n_1 - 1)^{l_1+1}, (n_2 + 1)^{l_2-1} | \hat{W}_1\cdot\hat{W}_2 | n_1^{l_1}, n_2^{l_2}\rangle = \sqrt{(N_1 - n_1 + 1)(N_2 - n_2)\left(\frac{n_1 - l_1}{2}\right)\left(\frac{n_2 - l_2}{2} + 1\right)}$$

$$\langle (n_1 - 1)^{l_1+1}, (n_2 - 1)^{l_2-1} | \hat{W}_1\cdot\hat{W}_2 | n_1^{l_1}, n_2^{l_2}\rangle = -\sqrt{(N_1 - n_1 + 1)(N_2 - n_2 + 1)\left(\frac{n_1 - l_1}{2}\right)\left(\frac{n_2 + l_2}{2}\right)} \quad (25)$$

and similar expressions with the index 1 interchanged with 2 on the left-hand side. It is seen that $\hat{W}_1\cdot\hat{W}_2$ has matrix elements that conserve the polyad number, similar to those of $\hat{M}_{12}$, and some which do not. This operator leads to cis-bent and trans-bent configurations.

2.5. Symmetry Adapted Basis. If only the nondiagonal operators $\hat{M}_{12}$ and $\hat{Q}_1\cdot\hat{Q}_2$ are kept in addition to the diagonal (Dunham-like) terms, the dimension of the matrix to diagonalize is still manageable, even for large $N = N_1 + N_2$, since then, the interactions conserve polyad number, $n_1 + n_2$. This is appropriate for linear molecules. However, in the general case in which the operators $\hat{W}_i^2$ and $\hat{W}_1\cdot\hat{W}_2$ are kept, one must diagonalize in

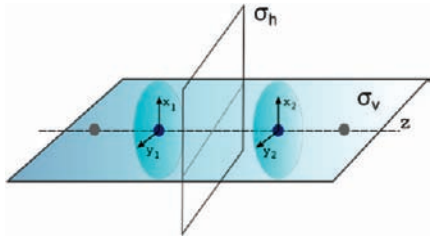

Figure 2. Schematic representation of the coordinate assignment and relevant symmetry operations in the linear case.

the full space and the dimension becomes very large. Even taking into account the fact that the total 2D angular momentum $l_{12} = l_1 + l_2$ is conserved, the dimension of the Hamiltonian blocks (for $N_1 = N_2 = N/2$) is

$$\dim(l_{12}) = \frac{1}{4}\sum_{l_1=l_{12}-N/2}^{N/2}(N/2 - |l_{12} - l_1| - \mathrm{mod}(N/2 - |l_{12} - l_1|, 2) + 2) \times (N/2 - |l_1| - \mathrm{mod}(N/2 - |l_1|, 2) + 2) \quad (26)$$

A reduction in the dimension of the blocks can be achieved by constructing a symmetry adapted basis. We use in this article the basis (Ia) and construct the symmetry adapted basis by using the so-called eigenfunction method of Chen,[23] adapted to molecular vibrations by Lemus.[24]

2.5.1. Linear Case, $D_{\infty h}$. In Figure 2, we show the coordinate assignments for a linear molecule with two benders. The symmetry here is $D_{\infty h}$, with irreducible representations (irreps) $\Sigma^{\pm}_{g/u}$ for $l_{12} = 0$, $\Pi_{g/u}$ for $l_{12} = 1$, $\Delta_{g/u}$ for $l_{12} = 2$, and so on.

The first step for building a symmetry-adapted basis consists in splitting the basis space into gerade and ungerade subspaces. To do so, we consider the transposition operator, (12), that permutes the two U(3) algebras. This symmetry operation corresponds to (σ_h), reflection through a plane perpendicular to the molecular axis,[25,26] as can be seen in Figure 2. The result of the application of the transposition operator to a local basis state is

$$(12)|n_1^{l_1}, n_2^{l_2}\rangle = |n_2^{l_2}, n_1^{l_1}\rangle \quad (27)$$

and, upon diagonalization of its associated matrix, one can separate the gerade (eigenvalue $\lambda = 1$) and ungerade (eigenvalue $\lambda = -1$) subspaces. This is enough to treat the $l_{12} \neq 0$ cases. Each Hamiltonian block, $H_{l_{12}}$, is split into its gerade and ungerade components as

$$H^{g}_{l_{12}} = G \cdot H_{l_{12}} \cdot G^{t}$$
$$H^{u}_{l_{12}} = U \cdot H_{l_{12}} \cdot U^{t} \quad (28)$$

where G and U are the orthonormal bases formed with the eigenvectors of the transposition operator with eigenvalues $\lambda = 1$ and $\lambda = -1$, respectively.

The Σ case ($l_{12} = 0$) requires further work to assign the $\pm$ labels. The relevant symmetry operation in this case is (σ_v), the reflection plane that contains the molecular axis.[27] As shown in Figure 2, the action of (σ_v) on the coordinates leaves x_s invariant

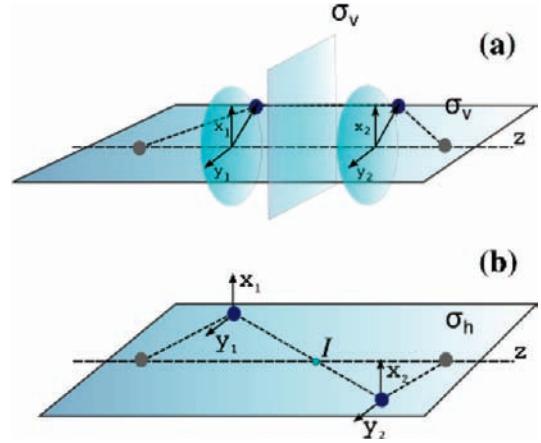

Figure 3. Schematic representation of the coordinate assignment and relevant symmetry operations in the nonlinear cases. Panel a, symmetry C_{2v} cis configuration. Panel b symmetry C_{2h} trans configuration.

and changes the sign of y_s ($s = 1, 2$). For circular boson operators, this implies

$$(\sigma_v)\tau^{\dagger}_{s,\pm}(\sigma_v) = -\tau^{\dagger}_{s,\mp}, \qquad s = 1, 2 \quad (29)$$

Using eq 14

$$(\sigma_v)|n_1^{l_1}, n_2^{l_2}\rangle = (-1)^{n_1+n_2}|n_1^{-l_1}, n_2^{-l_2}\rangle \quad (30)$$

In particular, for $l_{12} = 0$, the former equation reduces to

$$(\sigma_v)|n_1^{l}, n_2^{-l}\rangle = |n_1^{-l}, n_2^{l}\rangle \quad (31)$$

as $l_1 = -l_2$ and the number of quanta n_1 and n_2 have the same parity. If the matrix **S** defined by the action of the (σ_v) operator is constructed, it can be first split into gerade and ungerade components as in eq 28.

The eigenfunctions of S^g (S^u) associated with the eigenvalue $\lambda = 1(-1)$ correspond to $\Sigma^{\pm}_g$ ($\Sigma^{\pm}_u$) and form an orthonormal invariant subspace. Finally, the Σ Hamiltonian matrix block for Σ states is divided into four sub-blocks

$$H^{g,\pm}_{l_{12}=0} = G_{\pm} \cdot H^{g}_{l_{12}=0} \cdot G^{t}_{\pm}$$
$$H^{u,\pm}_{l_{12}=0} = U_{\pm} \cdot H^{u}_{l_{12}=0} \cdot U^{t}_{\pm} \quad (32)$$

where $G_{\pm}$ and $U_{\pm}$ are the orthonormal bases formed with the eigenvectors of the transposition operator (12) and of (σ_v).

2.5.2. Cis-Bend and Trans-Bend Cases, C_{2v} and C_{2h}. Panels a and b of Figure 3 show these configurations. In the first case, cis configuration, the molecular point symmetry group is C_{2v}, and the symmetry operations necessary to assign symmetry labels to the states are the reflections $\sigma_v(xz)$ and $\sigma_v(yz)$, shown in panel a of Figure 3. Those two symmetry operations can be mapped to (σ_v) and (σ_h) of the linear case. The irreps involved for every value of l are A_1, A_2, B_1, and B_2. They are associated with eigenvalue pairs ((12), (σ_v)) = (1, 1), (−1, −1), (−1, 1), and (1, −1) respectively.[23,25]

The second possible configuration is a trans configuration, with C_{2h} symmetry, depicted in panel b of Figure 3. The relevant symmetry operations in this case are the reflection plane (σ_h), which corresponds to the (σ_v) reflection plane in the linear

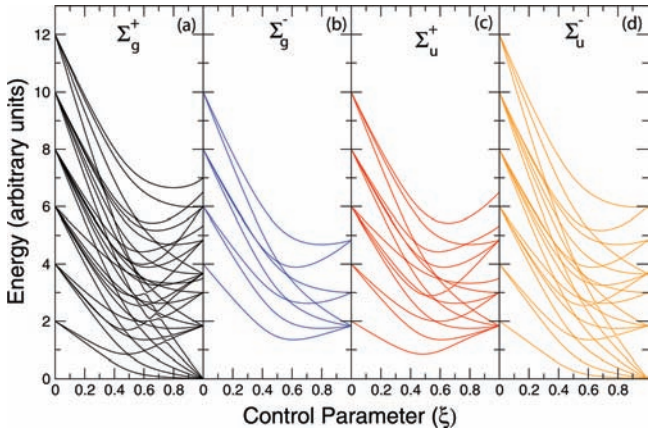

Figure 4. Correlation energy diagram for $N_1 = N_2 = 6$, and vibrational angular momentum $l_{12} = 0$. The control parameter $\eta = 0$. Panels a−d correspond to symmetries Σ_g^+, Σ_g^-, Σ_u^+, and Σ_u^- in the linear limit.

configuration, and the inversion (I). In the last case the action of (I) upon basis states results in

$$(I)|n_1^{l_1},n_2^{l_2}\rangle = (-1)^{n_1+n_2}|n_2^{l_2},n_1^{l_1}\rangle \tag{33}$$

These two operators should be diagonalized and the possible irreps are A_g, A_u, B_g, and B_u with eigenvalues (1, 1), (−1, −1), (−1, 1), and (1, −1).

2.5.3. Nonplanar Case, C_2. The construction of the symmetry adapted basis for this case will not be reported here, but it will be presented in a forthcoming publication.

3. Correlation Diagrams. The main advantage of the algebraic formulation is that one can describe, within the same framework, all configurations, linear, cis-bent, trans-bent, and nonplanar with local and normal behavior as well as intermediate situations. This aspect is best shown by constructing correlation diagrams, that is, diagrams in which the energy levels are followed from one limiting case to the other. Correlation diagrams from local to normal were constructed long ago and reported in refs 19 and 28. Here we show the correlation diagrams linear−cis-bent and linear−trans-bent.

To construct these correlation diagrams, we diagonalize a simplified Hamiltonian

$$\hat{H}^{(\mathrm{Ia-IIb})} = \varepsilon'\left((1-\xi)[\hat{n}_1+\hat{n}_2] + \xi\left[\frac{\hat{P}_1+\hat{P}_2}{N} + 2\eta\frac{\hat{W}_1\cdot\hat{W}_2}{N}\right]\right) \tag{34}$$

where $\hat{P}_i = N_i(N_i+1) - \hat{W}_i^2$. This Hamiltonian, called the essential Hamiltonian in the theory of quantum phase transitions, contains Casimir operators of chain Ia (linear) and IIb (bent-coupled). It corresponds to $\alpha = \alpha_{12} = \beta = \beta_{12} = \lambda = B = 0$ in eq 10 and $\varepsilon = \varepsilon'(1-\xi)$, $A = \varepsilon'\xi/N$, and $A_{12} = 2\varepsilon'\xi\eta/N$. The parameters ξ and η are called control parameters. The parameter ξ determines the structure linear-bent, while the parameter η determines the nature of the coupling between the two benders, $\eta > 0$ trans-bent, $\eta < 0$ cis-bent. In Figure 4, Figure 5, and Figure 6, we show the correlation diagram for states with $l_{12} = 0$ (Σ states in the linear limit), for a fixed value of $\eta = 0, \pm 1$. These correlation diagrams were also shown in ref 17 in a slightly different form. In Figure 4, all states are doubly degenerate since there is no interaction between the two benders, $\eta = 0$.

It is instructive to show also the correlation diagram for states with $l_{12} = 1$ (Π states in the linear limit), given in Figure 7, Figure 8, and Figure 9. Again, in Figure 7, all the states are doubly degenerate. One can see that the transition from linear to bent is characterized by a softening of the Π mode (Π_g for transition to cis-bent and Π_u for transition to trans-bent). The energy of the Π states becomes zero in the bent limit, since these states become part of the rotational ground state band.[29]

In addition to showing that all situations, linear, cis-bent, trans-bent, local, and normal can be described in a simple framework, correlation diagrams are also useful to study quantum phase transitions, that is, phase transitions that occur as a function of a coupling constant, here ξ, rather than the temperature. These transitions were investigated for a single bender in ref 16. They can occur both at zero energy, i.e., in the ground state, and at higher energies. In the last case they are known as excited state quantum phase transitions (ESQPT)[30] and are particularly interesting. For example, the water molecule, with a single bender, appears to undergo an

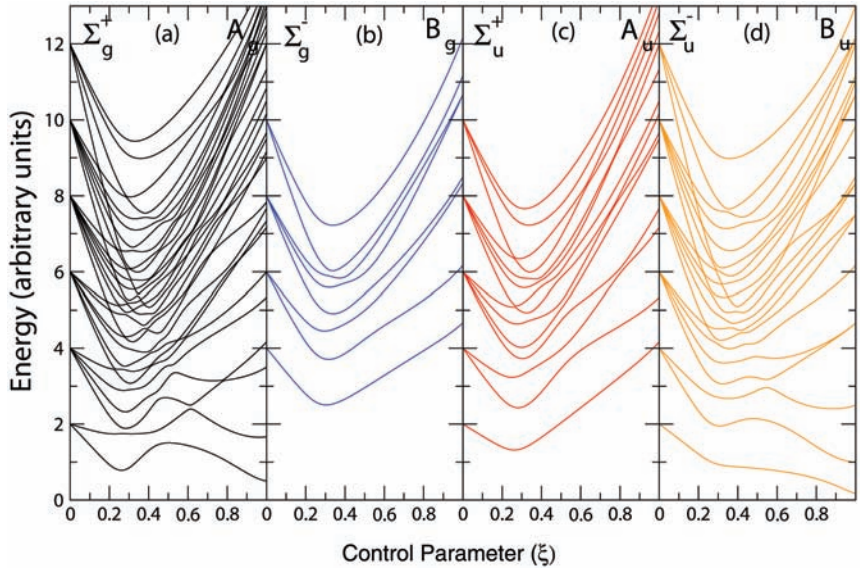

Figure 5. Correlation energy diagram for $N_1 = N_2 = 6$, and vibrational angular momentum $l_{12} = 0$. The control parameter $\eta = 1$. Both the linear, Σ_g^+, Σ_g^-, Σ_u^+, Σ_u^-, and trans-bent, A_g, B_g, B_u, A_u, symmetry labels are indicated.

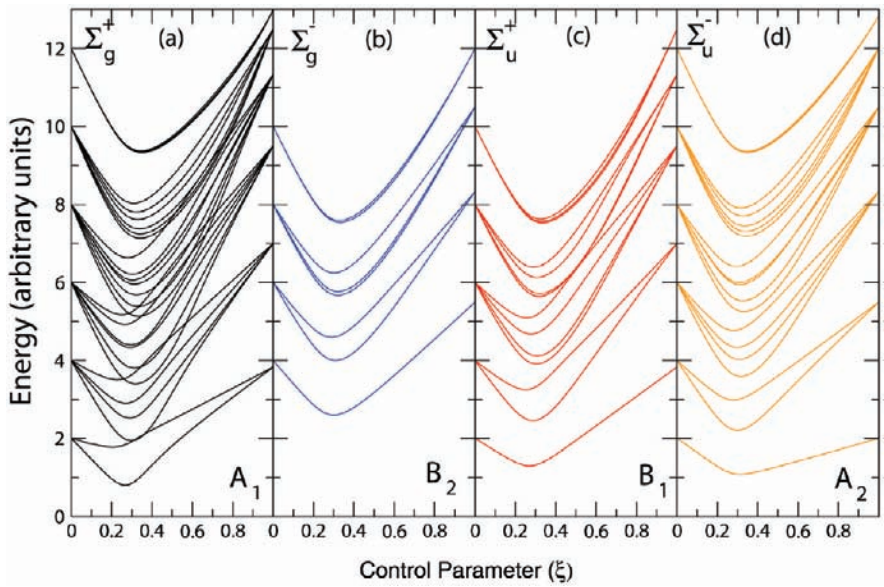

Figure 6. Correlation energy diagram for $N_1 = N_2 = 6$, and vibrational angular momentum $l_{12} = 0$. The control parameter $\eta = -1$. Both the linear, Σ_g^+, Σ_g^-, Σ_u^+, Σ_u^-, and cis-bent, A_1, B_2, B_1, A_2, symmetry labels are indicated.

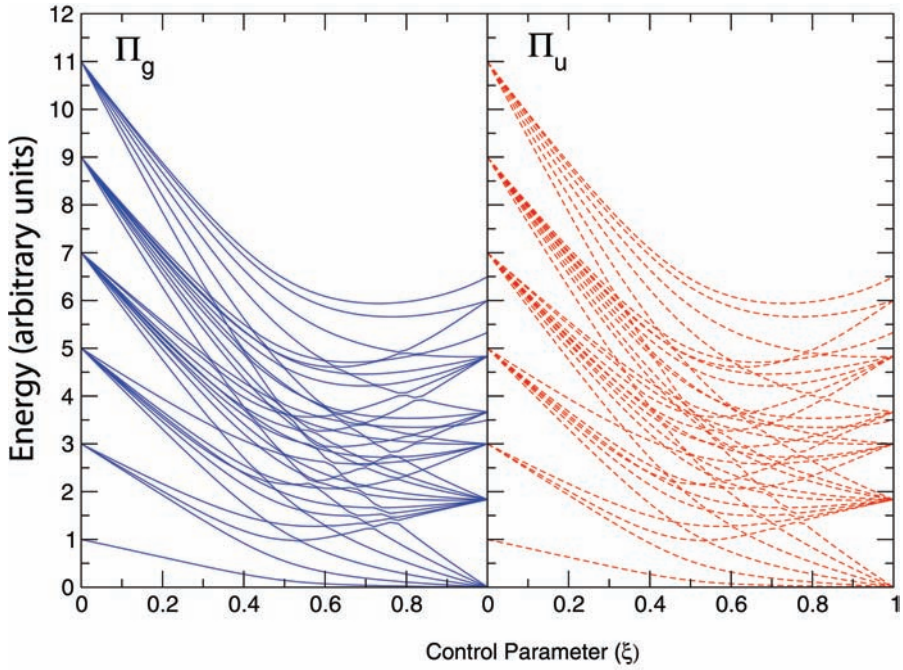

Figure 7. Correlation energy diagram for $N_1 = N_2 = 6$, and vibrational angular momentum $l_{12} = 1$. The control parameter $\eta = 0$. Left and right panels correspond to symmetries Π_g and Π_u in the linear limit.

ESQPT from bent to linear around 11 000 cm^{-1}.[31] For coupled benders, one can have two types of QPT or ESQPT, normal−local or linear−bent. The transition normal to local appears to occur in C_2H_2 at ≈15 000 cm^{-1}.[32] This transition can be related to the appearance of new modes born in the bifurcation of traditional normal modes.[11] The physical insight into this problem can be enlarged using catastrophe theory.[12] An appealing subject for future developments is the study of the possible relationship between ESQPT and bifurcations in classical Hamiltonians.

4. Semiclassical Analysis and Potential Functions. The algebraic expansion of the Hamiltonian $\hat{H}$ of eq 10 is similar to the Dunham-like expansion plus perturbations commonly used in molecular spectroscopy.[3] An alternative method of analysis is the force field expansion[1,2,10] in which the Hamiltonian is written in terms of coordinates and momenta. This expansion can be retrieved from the algebraic Hamiltonian by the method of coherent (or intrinsic) states. One introduce the states

$$|[N_1][N_2];r_1,\theta_1;r_2,\theta_2\rangle = \frac{1}{\sqrt{N_1!N_2!}}(b_{c,1}^{\dagger})^{N_1}(b_{c,2}^{\dagger})^{N_2}|0\rangle \qquad (35)$$

where (r_i, θ_i) are the polar coordinates associated with x_i, y_i $(i = 1, 2)$, in Figure 2,

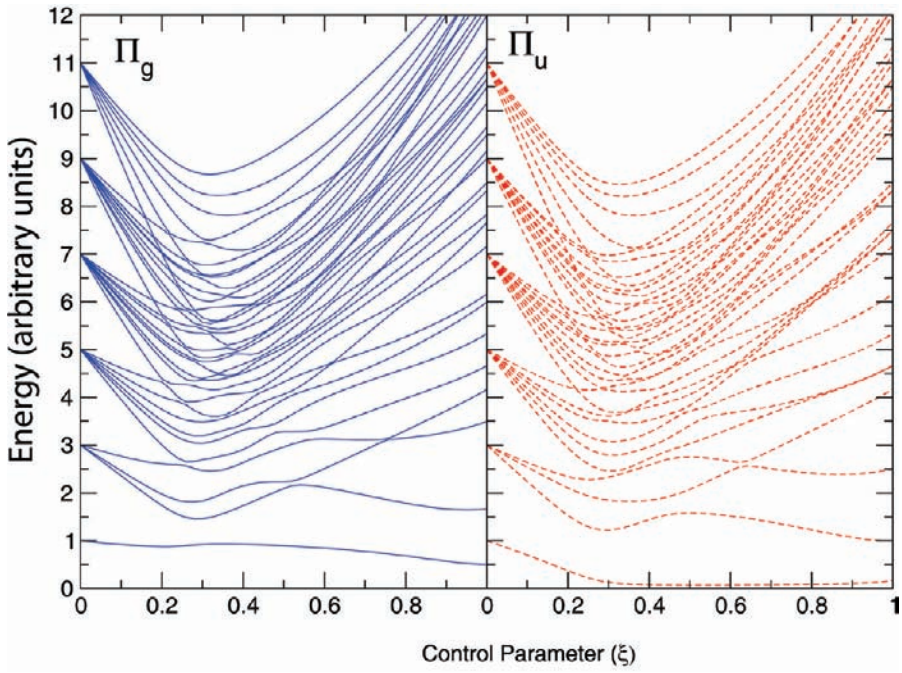

Figure 8. Correlation energy diagram for $N_1 = N_2 = 6$, and vibrational angular momentum $l_{12} = 1$. The control parameter $\eta = 1$. Left and right panels correspond to symmetries Π_g and Π_u in the linear limit.

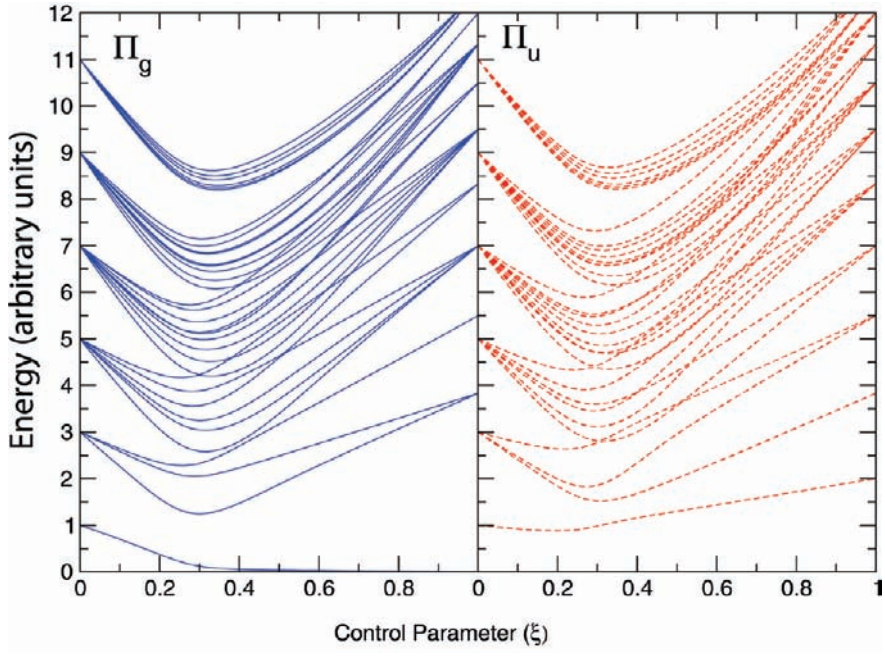

Figure 9. Correlation energy diagram for $N_1 = N_2 = 6$, and vibrational angular momentum $l_{12} = 1$. The control parameter $\eta = -1$. Left and right panels correspond to symmetries Π_g and Π_u in the linear limit.

$$\begin{cases} x_i = r_i \cos\theta_i \\ y_i = r_i \sin\theta_i \end{cases} \tag{36}$$

$$b^{\dagger}_{c,i} = \frac{1}{\sqrt{1+r^2}}[\sigma^{\dagger}_i + (x_i\tau^{\dagger}_{i,x} + y_i\tau^{\dagger}_{i,y})] \tag{37}$$

The states (35) will be simply denoted by $|r_1, \theta_1; r_2, \theta_2\rangle$ in the following paragraphs.

Operators $b^{\dagger}_{c,i}$ are the creation operators for the ith boson condensate

These coherent states were originally introduced in the study of nuclei[33−36] and adapted later to molecular systems.[37−41] The parameters (r_i, θ_i) in the coherent state are in general complex and represent coordinates and momenta.[40,41] In this article, we consider only the dependence on coordinates and thus put all momenta, $p_{r,i}$, $p_{\theta,i}$, $i = 1, 2$, equal to zero.[19]

The expectation values of the operators appearing in the general Hamiltonian, eq 10, in the intrinsic state are

$$
\begin{aligned}
&\langle r_1,r_2,\phi|\hat{n}_1+\hat{n}_2|r_1,r_2,\phi\rangle = \frac{N}{2}\sum_{i=1}^{2}\frac{r_i^2}{1+r_i^2}\\
&\langle r_1,r_2,\phi|\hat{n}_1(\hat{n}_1+1)+\hat{n}_2(\hat{n}_2+1)|r_1,r_2,\phi\rangle =\\
&\qquad N\sum_{i=1}^{2}\left\{\frac{N/2-1}{2}\frac{r_i^2}{1+r_i^2}+1\right\}\frac{r_i^2}{1+r_i^2}\\
&\langle r_1,r_2,\phi|\hat{n}_1\hat{n}_2|r_1,r_2,\phi\rangle = \frac{N^2}{4}\frac{r_1^2r_2^2}{(1+r_1^2)(1+r_2^2)}\\
&\langle r_1,r_2,\phi|\hat{l}_1^2+\hat{l}_2^2|r_1,r_2,\phi\rangle = \frac{N}{2}\sum_{i=1}^{2}\frac{r_i^2}{1+r_i^2}\\
&\langle r_1,r_2,\phi|\hat{l}_1\hat{l}_2|r_1,r_2,\phi\rangle = 0\\
&\langle r_1,r_2,\phi|\hat{M}_{12}|r_1,r_2,\phi\rangle = \frac{N^2}{4}\left[\sum_{i=1}^{2}\frac{r_i^2}{1+r_i^2}-2\prod_{i=1}^{2}\frac{r_i^2}{1+r_i^2}-8\left(\prod_{i=1}^{2}\frac{r_i}{1+r_i^2}\right)\cos(\phi)\right]\\
&\langle r_1,r_2,\phi|\hat{P}_1+\hat{P}_2|r_1,r_2,\phi\rangle = \frac{N(N-2)}{4}\sum_{i=1}^{2}\left(\frac{1-r_i^2}{1+r_i^2}\right)^2\\
&\langle r_1,r_2,\phi|2\hat{W}_1\cdot\hat{W}_2|r_1,r_2,\phi\rangle = 2N^2\left(\prod_{i=1}^{2}\frac{r_i}{1+r_i^2}\right)\cos(\phi)\\
&\langle r_1,r_2,\phi|\hat{Q}_1\cdot\hat{Q}_2|r_1,r_2,\phi\rangle = \frac{N^2}{4}\left(\prod_{i=1}^{2}\frac{r_i^2}{1+r_i^2}\right)\cos(2\phi)
\end{aligned}
\tag{38}
$$

where $N_1 = N_2 = N/2$ for ABBA molecules. These expectation values depend only on the dihedral angle between the two B−B−A groups, $\phi = \theta_1 - \theta_2$, and hence the intrinsic states have been written in 38 as $|r_1, r_2, \phi\rangle$. The expectation value of the Hamiltonian 10 in the intrinsic state gives the ground state energy functional, $E(r_1, r_2, \phi)$, or potential function

$$
\begin{aligned}
E(r_1,r_2,\phi) &= \frac{\langle \text{i.s.}|\hat{H}|\text{i.s.}\rangle}{N} \equiv V(r_1,r_2,\phi)\\
&= \frac{\varepsilon}{2}\sum_{i=1}^{2}\frac{r_i^2}{1+r_i^2}+\frac{\beta}{2}\sum_{i=1}^{2}\frac{r_i^2}{1+r_i^2}+\\
&\quad \alpha\sum_{i=1}^{2}\left(\frac{(N/2-1)}{2}\frac{r_i^2}{1+r_i^2}+1\right)\frac{r_i^2}{1+r_i^2}+\alpha_{12}\frac{N}{4}\frac{r_1^2r_2^2}{(1+r_1^2)(1+r_2^2)}+\\
&\quad A\frac{(N-2)}{4}\sum_{i=1}^{2}\left(\frac{1-r_i^2}{1+r_i^2}\right)^2+2A_{12}N\left(\prod_{i=1}^{2}\frac{r_i}{1+r_i^2}\right)\cos(\phi)+\\
&\quad \lambda\frac{N}{4}\left[\sum_{i=1}^{2}\frac{r_i^2}{1+r_i^2}-2\prod_{i=1}^{2}\frac{r_i^2}{1+r_i^2}-8\left(\prod_{i=1}^{2}\frac{r_i}{1+r_i^2}\right)\cos(\phi)\right]+\\
&\quad B\frac{N}{4}\left(\prod_{i=1}^{2}\frac{r_i^2}{1+r_i^2}\right)\cos(2\phi)
\end{aligned}
\tag{39}
$$

This expansion of the potential function is similar in spirit to the conventional expansion, for example as given in ref 42. The potential function (39) depends on the displacements (r_1, r_2) of the benders from the molecular axis of Figure 2 and on the dihedral angle ϕ.

The equilibrium configuration of the molecule is obtained by minimizing $E(r_1, r_2, \phi)$ with respect to the variables r_1, r_2, and ϕ. For ABBA molecules we can put $r_{1e} = r_{2e} = r_e$. This equilibrium configuration depends on the values of the parameters.

One can see that the potential function (39) includes the following cases: (a) $r_e = 0$ (linear configuration, Figure 1a); (b) $r_e \neq 0$, $\phi = 0$, the benders are displaced in the same direction (planar cis-configuration, Figure 1b); (c) $r_e \neq 0$, $\phi = \pi$, the benders are

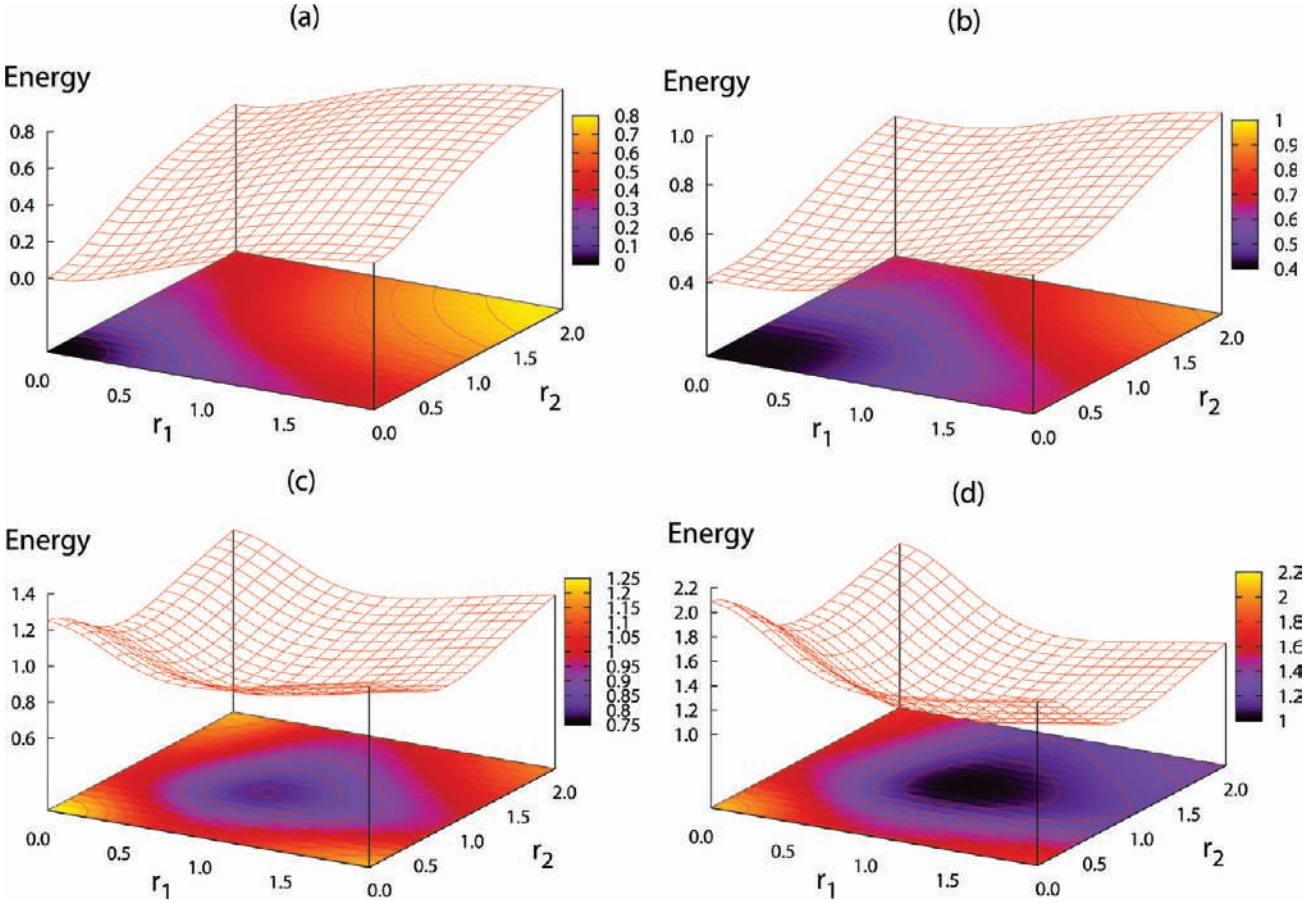

Figure 10. Potential surfaces (arbitrary units) as a function of r_1 and r_2 for fixed $\phi = 0°$. Panel a: $\xi = 0.0$. Panel b: $\xi = 0.2$, $\eta = -1.0$. Panel c: $\xi = 0.6$, $\eta = -1.0$. Panel d: $\xi = 1.0$, $\eta = -1.0$. In all cases, $N = 50$.

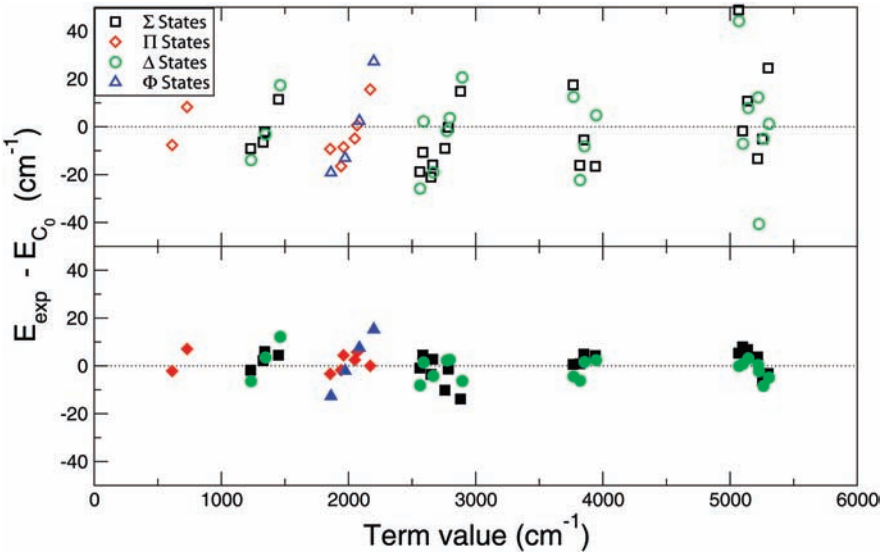

Figure 11. Residuals for the fits H_0 (upper panel, open symbols) and H_3 (lower panel, filled symbols) to C_2H_2 experimental bending term values below 6000 cm^{-1}.

displaced in opposite directions (planar trans-configuration, Figure 1c); (d) $r_e \neq 0, \phi \neq 0, \pi$ (nonplanar configuration, Figure 1d).The last case occurs only if the coefficient B in eq 39 is different from zero, as first discussed in ref 18; equilibrium values of ϕ different from 0, π arise from the competition between the term in $\cos(\phi)$ and the term in $\cos(2\phi)$. The maximal nonplanarity is for $\phi = \pi/2$.

To visualize how the transitions from linear to bent occurs in the potential function, it is convenient to consider the simplified Hamiltonian (34). In this case the potential function is

$$E(r_1,r_2,\phi) = \frac{\langle r_1,r_2,\phi|\hat{H}^{(\mathrm{Ia-IIb})}|r_1,r_2,\phi\rangle}{\varepsilon' N} \equiv \mathcal{V}(r_1,r_2,\phi)$$

$$= (1-\xi)\left[\frac{1}{2}\sum_{i=1}^{2}\frac{r_i^2}{1+r_i^2}\right] + \xi\left[\frac{(N-2)}{4N}\times \sum_{i=1}^{2}\left(\frac{1-r_i^2}{1+r_i^2}\right)^2 + 2\eta\left(\prod_{i=1}^{2}\frac{r_i}{1+r_i^2}\right)\cos(\phi)\right] \quad (40)$$

This function is shown in Figure 10 for $\phi = 0$ and $\xi = 0.0$, 0.2, 0.6, and 1.0 and $\eta = -1$. The minimum shifts from $r_{1e} = r_{2e} = 0$ at $\xi = 0$ (linear) to $r_{1e} = r_{2e} = 1$ at $\xi = 1$ (cis-bent). The displacements r_{1e}, r_{2e} are here dimensionless. To compare with ab initio calculations of the potential energy surface, one needs to introduce a scale S as in ref 14. A similar figure can be constructed for trans-bent configurations with $\eta = 1.0$.

The simplified potential function (40) is amenable to the study of quantum phase transitions. There are two control parameters, ξ and η, and the phase diagram is two-dimensional. A preliminary account of linear−cis-bent and linear−trans-bent phase transitions was given in ref 17. Quantum phase transitions can also be studied by means of catastrophe maps.[11,12] For the simplified Hamiltonian (34) the catastrophe map is a plane and it corresponds to the catastrophe map of a single resonance discussed in refs 11 and 12. The two control parameters ξ and η are equivalent to the two control parameters A_1 and A_3 of ref 12. For the general potential function (39) there are more control parameters and the phase diagram (and its corresponding catastrophe map) are multidimensional. A study of multidimensional phase diagrams has been done within the framework of algebraic models in nuclear physics.[43,44] The study of multidimensional catastrophe maps has been recently proposed by Tyng and Kellman[12] in the treatment of bending vibrations of acetylene. A multidimensional study for the full algebraic Hamiltonian (10) will be presented elsewhere.

5. Sample Calculation: Bending Vibrations of C_2H_2 ($\tilde{X}^1\Sigma^+$). To illustrate the algebraic approach to bending vibrations in tetratomic molecules, we perform here a calculation of acetylene, C_2H_2, in its electronic ground state $\tilde{X}^1\Sigma^+$. We consider a total number of 53 term values below 6000 cm^{-1} taken from refs 4, 10, 42, 45, 47, and 48. The parameter optimization is obtained using the Minuit package.[46] All fits are done within a model space with $N_1 = N_2 = 20$. The parameter values obtained including different physically relevant operators are given in Table 1.

One can see from these fits that one can obtain a description of the 53 levels with rms = 17.1 cm^{-1} in terms of only three parameters, ε, β, and λ. The introduction of the parameter B (l-resonance) brings the rms down to 11.2 cm^{-1}. Not much is

TABLE 1: Parameters Obtained from Fits to the Available Experimental Bending Energy Levels below 6000 cm^{-1} for C_2H_2 with the Two-Body Algebraic Hamiltonian, eq 10, with $N_1 = N_2 = 20$ and Different Subsets of the Available Parameters[a]

param	H_0	H_1	H_2	H_3
ε	667.27(6)	665.73(7)	598.8(27)	667.98(15)
α			3.33(13)	−1.68(3)
α_{12}				6.46(10)
β	4.03(5)	5.09(5)	3.53(9)	4.54(6)
β_{12}				2.02(14)
λ	−2.539(3)	−2.649(4)	−2.669(4)	−2.705(4)
A			1.66(6)	
A_{12}				
B		3.52(4)	3.61(4)	4.10(5)
rms	17.1	11.2	11.1	6.1

[a] A total number of 53 term values were included. Numbers in parentheses denote one standard deviation of the least squares fit assuming equal error for all experimental levels. Parameters and rms are in units of cm^{-1}.

TABLE 2: Bending C_2H_2 Experimental Term Values and Residuals Associated with the Calculations H_0, H_1, and H_3 Whose Parameters are Given in Table 1[a]

l_{12}	Γ	$(v_4^{l_4}, v_5^{l_5})$	E_{exp}[4,10,42,45,47,48]	Exp − E_{H_0}	Exp − E_{H_1}	Exp − E_{H_3}
0	Σ_g^+	$2^0 0^0$	1230.39	−9.11	−6.05	−1.80
0	Σ_g^+	$0^0 2^0$	1449.11	11.48	5.39	4.47
0	Σ_g^+	$2^2 2^2$	2648.02	−21.06	−10.24	−3.55
0	Σ_g^+	$0^0 4^0$	2880.22	14.84	−4.56	−13.87
0	Σ_g^+	$6^0 0^0$	3765.99	17.48	6.76	0.60
0	Σ_g^+	$4^0 2^0$	3940.48	−16.52	1.65	4.33
0	Σ_g^+	$8^0 0^0$	5066.97	48.86	21.98	5.31
0	Σ_g^+	$6^0 2^0$	5216.22	−13.34	8.88	3.73
0	Σ_g^-	$2^2 2^2$	2661.19	−15.94	2.18	2.76
0	Σ_u^+	$1^1 1^1$	1328.08	−6.46	−3.38	2.20
0	Σ_u^+	$1^3 1^1$	2757.80	−9.03	−15.71	−10.18
0	Σ_u^+	$3^1 1^1$	2560.60	−18.79	−16.02	−0.93
0	Σ_u^+	$5^1 1^1$	3818.43	−16.12	−20.10	0.88
0	Σ_u^+	$7^1 1^1$	5098.38	−1.76	−18.59	7.99
0	Σ_u^+	$5^1 3^1$	5254.53	−5.13	14.24	−6.35
0	Σ_u^-	$1^1 1^1$	1340.55	−2.04	5.96	5.99
0	Σ_u^-	$1^3 1^1$	2783.65	−0.24	1.83	−1.31
0	Σ_u^-	$3^1 1^1$	2583.84	−10.69	3.01	4.55
0	Σ_u^-	$5^1 1^1$	3850.32	−5.52	8.84	4.92
0	Σ_u^-	$7^1 1^1$	5137.37	10.75	21.58	6.81
0	Σ_u^-	$5^1 3^1$	5298.93	24.55	2.78	−3.19
1	Π_g	$1^1 0^0$	612.87	−7.65	−4.97	−2.18
1	Π_g	$1^1 2^0$	2049.06	−4.93	−1.20	2.47
1	Π_g	$1^1 2^2$	2066.99	0.60	3.02	5.71
1	Π_g	$3^1 0^0$	1855.72	−9.28	−6.94	−3.34
1	Π_u	$0^0 1^1$	730.33	8.26	6.53	7.06
1	Π_u	$2^2 1^1$	1941.18	−16.51	−8.43	−1.77
1	Π_u	$2^0 1^1$	1960.87	−8.55	−0.88	4.43
1	Π_u	$0^0 3^1$	2170.34	15.60	4.16	6.37
2	Δ_g	$2^2 0^0$	1233.52	−14.03	−9.81	−6.40
2	Δ_g	$0^0 2^2$	1463.02	17.33	12.87	12.12
2	Δ_g	$2^2 2^0$	2666.15	−19.03	−20.57	−4.24
2	Δ_g	$0^0 4^2$	2894.07	20.64	2.86	−6.30
2	Δ_g	$6^2 0^0$	3769.12	12.57	2.91	−4.39
2	Δ_g	$4^0 2^2$	3947.38	4.83	−0.71	2.38
2	Δ_g	$8^2 0^0$	5070.31	44.17	18.28	−5.96
2	Δ_g	$6^0 2^2$	5221.83	12.32	5.96	0.34
2	Δ_u	$1^1 1^1$	1347.52	−3.12	−4.31	3.50
2	Δ_u	$3^3 1^1$	2561.53	−25.84	−12.77	−8.10
2	Δ_u	$3^1 1^1$	2589.68	2.31	−7.76	1.45
2	Δ_u	$1^1 3^3$	2773.19	−1.75	2.64	2.28
2	Δ_u	$1^1 3^1$	2795.50	3.62	−1.63	2.53
2	Δ_u	$5^3 1^1$	3820.24	−22.25	−15.79	−6.13
2	Δ_u	$5^1 1^1$	3855.82	−8.16	−2.62	1.60
2	Δ_u	$7^3 1^1$	5100.92	−7.13	−12.02	0.80
2	Δ_u	$7^1 1^1$	5142.62	7.86	8.13	3.11
2	Δ_u	$5^1 3^1$	5226.71	−40.65	11.05	−2.32
2	Δ_u	$5^1 3^3$	5262.39	−4.98	−16.91	−8.44
2	Δ_u	$5^1 3^1$	5306.21	1.21	−4.01	−4.88
3	Φ_g	$3^3 0^0$	1861.93	−19.17	−14.54	−12.69
3	Φ_g	$1^1 2^2$	2084.85	2.44	−3.68	7.54
3	Φ_u	$2^2 1^1$	1972.59	−13.03	−14.71	−2.07
3	Φ_u	$0^0 3^3$	2198.13	27.29	19.09	15.24

[a] All energies are in cm^{-1}.

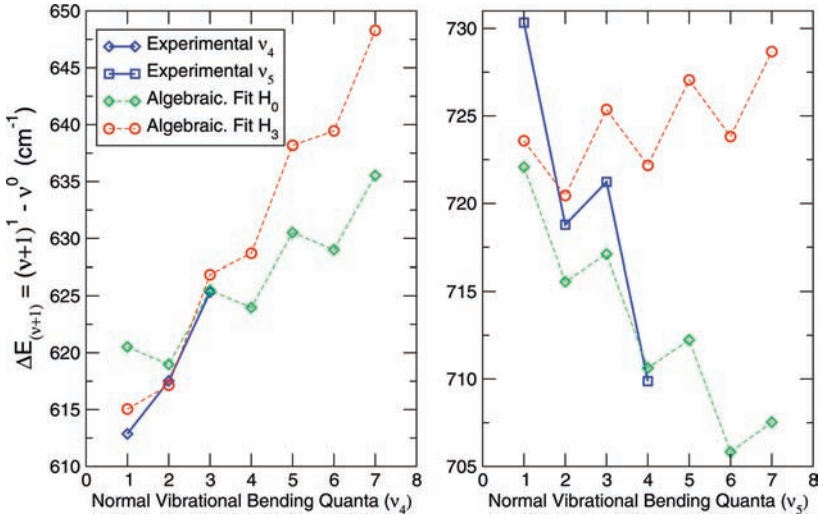

Figure 12. Birge−Sponer plot for ν_4 and ν_5 overtones. Available experimental data and results of calculations H_0 and H_3 are shown.

gained by the introduction of the (polyad breaking) parameter A (fit H_2 compared to fit H_1). Inclusion of additional parameters α, α_{12}, β_{12} brings the deviation down to 6.1 cm^{-1}. Finally, for C_2H_2 ($\tilde{X}^1\Sigma^+$) the parameters λ and A_{12} appear to have the same effect, as one can also see by the potential function they produce (see 39).

The values of the parameters in Table 1 support a linear normal configuration for C_2H_2 ($\tilde{X}^1\Sigma^+$) in its lowest part (<6000 cm^{-1}) of the spectrum. No polyad breaking terms appear to be important in this case. Polyad breaking terms play an important role only when bent configurations are studied.

Table 2 shows the experimental term values and the residuals $\Delta E = E_{exp} - E_{calc}$ obtained in calculations H_0, H_1, and H_3.

The results of the fit labeled H_0 (three parameters) are analyzed in the top portion of Figure 11 and those of fit H_3 (seven parameters) in the bottom portion of Figure 11. The discrepancies imply that higher order terms (cubic and quartic) are missing in the Hamiltonian of eq 10, a result also obtained in the Dunham-like expansion plus resonances. Higher order terms can be easily introduced in the algebraic approach, as discussed in refs 10 and 13, but their effects will not be presented here. We concentrate instead on some unusual features of the bending vibrations of acetylene, as emphasized by Birge−Sponer plots. The anharmonicities of the gerade Π_g vibration are positive, while those of the ungerade Π_u vibration are negative, as shown in Figure 12. The simple three parameter calculation, labeled H_0 in Table 1, produces anharmonicities which are positive for the gerade vibration and negative for the ungerade. In addition, the Birge−Sponer plot of the ungerade vibration has a marked odd−even staggering. This staggering is not clearly visible in the gerade vibrations, partly due to the fact that the term value of the $\nu_4 = 4$ state in not known for the gerade vibration. In fit H_3, the situation improves for the gerade vibration but becomes worse for the ungerade vibration. This again indicates that higher order terms may be needed.

Odd−even staggering is an important feature of bending vibrations, as it indicates a tendency toward instability leading to a cis or trans bent configuration. To display the instability, we show in Figure 13 the Birge−Sponer plot of the gerade vibration ν_4 obtained using the simplified Hamiltonian eq (34) for $\eta = -1$ and $\xi = 0$, 0.1, 0.2, 0.3. One can see from this figure how the staggering increases with ξ.

6. Summary and Discussion. In this article, we have presented an algebraic approach to coupled benders, capable

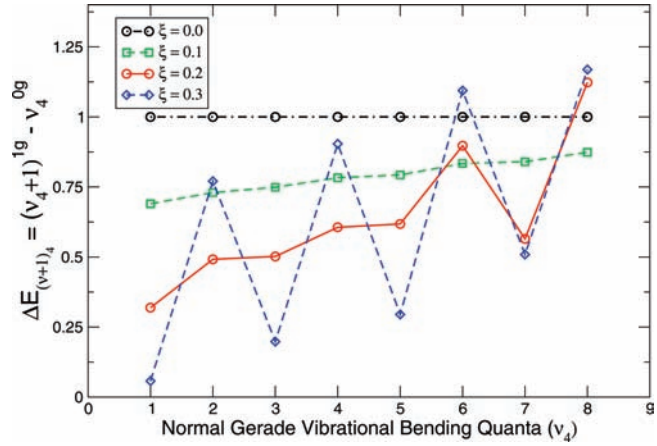

Figure 13. Birge−Sponer plot for $N_1 = N_2 = 6$, $\xi = 0$, 0.1, 0.2, and 0.3. Only the states corresponding to pure overtones of the gerade vibrational bending mode are shown. The control parameter is $\eta = -1$.

of describing within the same framework, all situations, linear, cis-bent, trans-bent, and nonplanar, and applied it to a sample calculation of the pure bent spectrum of C_2H_2 in its ground electronic state $\tilde{X}^1\Sigma^+$. A 3-parameter fit of 53 term values below 6000 cm^{-1} gives a rms of 17.1 cm^{-1}, while a 7-parameter fit gives a rms of 6.1 cm^{-1}. These fits were done with a quadratic Hamiltonian. We are planning in the immediate future to include higher order terms, cubic and quartic, to bring down the deviation to spectroscopic accuracy ($\leq$1 cm^{-1}), as already shown in ref 13 where the introduction of one cubic $(\hat{n}_1 + \hat{n}_2)\hat{M}_{12}$ and one quartic $(\hat{l}_1^2 + \hat{l}_2^2)\hat{M}_{12}$ term brought the deviation down to $\approx$1 cm^{-1}, and, specially, in ref 9, where the introduction of two cubic and three quartic terms brought the deviation down to 0.06 cm^{-1}.

In view of the versatility of our approach, we plan to perform calculations of the trans-bent configuration of C_2H_2 in its excited electronic state $\tilde{A}^1A_u$, and most importantly of the nonplanar configuration in water peroxide (H_2O_2),[49] treated in part in ref 18.

The algebraic method is on one side directly connected with the Dunham-like plus resonances expansion and on the other side to the force field expansion. We are planning to compare the potential functions obtained from the algebraic approach with ab initio functions, when available, and with phenomenological force field functions.

Acknowledgment. F.P.B. thanks the Ministerio de Educación y Ciencia for a fellowship of the "José Castillejo" program and the Junta de Andalucía for financial support through contract no. P07-FQM-02962. This work was performed in part under the DOE Grant No. DE-FG-02-91ER40608. We thank Mark Caprio, Pavel Cejnar, José Enrique García-Ramos, and Andrea Vitturi for valuable comments and Patrick H. Vaccaro for many useful discussions.

This article is dedicated to Bob Field, who has pioneered the study of the dynamics of acetylene.

References and Notes

(1) Strey, G.; Mills, I. M. *J. Mol. Spectrosc.* **1976**, *59*, 103–115.
(2) Bramley, M. J.; Carter, S.; Handy, N. C.; Mills, I. M. *J. Mol. Spectrosc.* **1993**, *157*, 301–336.
(3) Jacobson, M. P.; O'Brien, J. P.; Silbey, R. J.; Field, R. W. *J. Chem. Phys.* **1998**, *109*, 121–133.
(4) Hoshina, K.; Iwasaki, A.; Yamanouchi, K.; Jacobson, M. P.; Field, R. W. *J. Chem. Phys.* **2001**, *114*, 7424–7442.
(5) Iachello, F.; Oss, S.; Lemus, R. *J. Mol. Spectrosc.* **1991**, *149*, 132–151.
(6) Iachello, F.; Manini, N.; Oss, S. *J. Mol. Spectrosc.* **1992**, *156*, 190–200.
(7) Iachello, F.; Oss, S.; Viola, L. *Mol. Phys.* **1993**, *78*, 545–559.
(8) Iachello, F.; Oss, S.; Viola, L. *Mol. Phys.* **1993**, *78*, 561–575.
(9) Abbouti Temsamani, M.; Champion, J.-M.; Oss, S. *J. Chem. Phys.* **1999**, *110*, 2893–2902.
(10) Amano, T.; Sako, T.; Hoshina, K.; Yamanouchi, K. *Chem. Phys. Lett.* **2003**, *375*, 576–582.
(11) Tyng, V.; Kellman, M. E. *J. Phys. Chem. B* **2006**, *110*, 18859–18871.
(12) Tyng, V.; Kellman, M. E. *J. Chem. Phys.* **2009**, *130*, 144311/1–14.
(13) Iachello, F.; Oss, S. *J. Chem. Phys.* **1996**, *104*, 6956–6963.
(14) Iachello, F.; Pérez-Bernal, F.; Vaccaro, P. H. *Chem. Phys. Lett.* **2003**, *375*, 309–320.
(15) Pérez-Bernal, F.; Santos, L. F.; Vaccaro, P. H.; Iachello, F. *Chem. Phys. Lett.* **2005**, *414*, 398–404.
(16) Pérez-Bernal, F.; Iachello, F. *Phys. Rev. A* **2008**, *77*, 032115/1–21.
(17) Iachello, F.; Pérez-Bernal, F. *Mol. Phys.* **2008**, *106*, 223–231.
(18) Champion, J.-M.; Abbouti Temsamani, M.; Oss, S. *Chem. Phys. Lett.* **1999**, *308*, 274–282.
(19) Iachello, F.; Levine, R. D. *Algebraic Theory of Molecules*; Oxford University Press: Oxford, U.K., 1995.
(20) Kellman, M. E.; Chen, G. *J. Chem. Phys.* **1991**, *95*, 8671–8672.
(21) van Roosmalen, O. S.; Benjamin, I.; Levine, R. D. *J. Chem. Phys.* **1984**, *81*, 5986–5997.
(22) Kellman, M. E. *J. Chem. Phys.* **1990**, *93*, 6630–6635.
(23) Chen, J.-Q. *Group Representation Theory for Physicists*; World Scientific: Singapore, 1989.
(24) Lemus, R. *Mol. Phys.* **2003**, *101*, 2511–2528.
(25) Hammermesh, M. *Group Theory and its Application to Physical Problems*; Dover: New York, 1989.
(26) Herzberg, G. *Molecular Spectra and Molecular Structure, Vol. II: Infrared and Raman Spectra of Polyatomic Molecules*; Van Nostrand Reinhold: New York, 1945.
(27) In this and in the following subsection σ_v and σ_h denote the symmetry operations, not the σ bosons.
(28) Thorson, W. R.; Nakagawa, I. *J. Chem. Phys.* **1960**, *33*, 994–1004.
(29) The finite value in Figure 9 is a finite N effect, which vanishes when $N \rightarrow \infty$.
(30) Caprio, M. A.; Cejnar, P.; Iachello, F. *Ann. Phys. (NY)* **2008**, *323*, 1106–1145.
(31) Zobov, N. F.; Shirin, S. V.; Polyansky, O. L.; Tennyson, J.; Coheur, P.-F.; Bernath, P. F.; Carleer, M.; Colin, R. *Chem. Phys. Lett.* **2006**, *414*, 193–197.
(32) Jacobson, M. P.; Silbey, R. J.; Field, R. W. *J. Chem. Phys.* **1999**, *110*, 845–859.
(33) Gilmore, R. *J. Math. Phys.* **1979**, *20*, 891–893.
(34) Ginocchio, J. N.; Kirson, M. W. *Phys. Rev. Lett.* **1980**, *44*, 1744–1747.
(35) Bohr, A.; Mottelson, B. R. *Phys. Scr.* **1980**, *22*, 468–474.
(36) Dieperink, A. E. L.; Scholten, O.; Iachello, F. *Phys. Rev. Lett.* **1980**, *44*, 1747–1750.
(37) van Roosmalen, O. S.; Dieperink, A. E. L. *Phys. Lett. B* **1981**, *100*, 299–304.
(38) van Roosmalen, O. S.; Dieperink, A. E. L. *Ann. Phys.* **1982**, *139*, 198–211.
(39) van Roosmalen, O. S.; Levine, R. D.; Dieperink, A. E. L. *Chem. Phys. Lett.* **1983**, *101*, 512–517.
(40) van Roosmalen, O. S. Ph.D. thesis, University of Groningen, The Netherlands, 1982.
(41) Benjamin, I.; Levine, R. D. *Chem. Phys. Lett.* **1985**, *117*, 314–320.
(42) Plíva, J. *J. Mol. Spectrosc.* **1972**, *44*, 165–182.
(43) Caprio, M. A.; Iachello, F. *Ann. Phys. (NY)* **2005**, *318*, 454–494.
(44) Arias, J. M.; Dukelsky, J.; García-Ramos, J. E. *Phys. Rev. Lett.* **2004**, *93*, 212501/1–4.
(45) Herman, M. *Mol. Phys.* **2007**, *105*, 2217–2241.
(46) James, F.; Winkler, M. http://www.cern.ch/minuit, 2004.
(47) Plíva, J. *J. Mol. Spectrosc.* **1972**, *44*, 145–164.
(48) Kabbadj, Y.; Herman, M.; DiLonardo, G.; Fusina, L. *J. Mol. Spectrosc.* **1991**, *150*, 535–565.
(49) Kuhn, B.; Rizzo, T. R.; Luckhaus, D.; Quack, M.; Suhm, M. A. *J. Chem. Phys.* **1999**, *111*, 2562–2587.

JP9040474